9484–9492 *Nucleic Acids Research, 2014, Vol. 42, No. 14* *Published online 16 July 2014*
doi: 10.1093/nar/gku593

Engineering modular and tunable genetic amplifiers for scaling transcriptional signals in cascaded gene networks

Baojun Wang[1,2,*], Mauricio Barahona[3] and Martin Buck[2]

[1]Centre for Synthetic and Systems Biology, School of Biological Sciences, University of Edinburgh, Edinburgh EH9 3JR, UK, [2]Department of Life Sciences, Faculty of Natural Sciences, Imperial College London, London SW7 2AZ, UK and [3]Department of Mathematics, Faculty of Natural Sciences, Imperial College London, London SW7 2AZ, UK

Received May 14, 2014; Revised June 19, 2014; Accepted June 20, 2014

ABSTRACT

Synthetic biology aims to control and reprogram signal processing pathways within living cells so as to realize repurposed, beneficial applications. Here we report the design and construction of a set of modular and gain-tunable genetic amplifiers in *Escherichia coli* capable of amplifying a transcriptional signal with wide tunable-gain control in cascaded gene networks. The devices are engineered using orthogonal genetic components (*hrpRS*, *hrpV* and P_{hrpL}) from the *hrp* (hypersensitive response and pathogenicity) gene regulatory network in *Pseudomonas syringae*. The amplifiers can linearly scale up to 21-fold the transcriptional input with a large output dynamic range, yet not introducing significant time delay or significant noise during signal amplification. The set of genetic amplifiers achieves different gains and input dynamic ranges by varying the expression levels of the underlying ligand-free activator proteins in the device. As their electronic counterparts, these engineered transcriptional amplifiers can act as fundamental building blocks in the design of biological systems by predictably and dynamically modulating transcriptional signal flows to implement advanced intra- and extra-cellular control functions.

INTRODUCTION

Signal processing circuits are widely used in electronic systems to modulate the electrical signal flows necessary to achieve particular desired applications. Similarly, cells employ sophisticated gene regulatory networks to continuously process biological signals for their survival and reproduction (1,2). A central aim of synthetic biology is to control and reprogram such signal processing pathways within living cells (3,4) so as to realize repurposed, beneficial applications ranging from disease diagnosis (5,6) and environment sensing (7) to chemical bioproduction (8). A fundamental building block in analog circuit design is the amplifier (9), which scales an input signal by a factor known as the *amplification gain* (β^T), defined as the ratio between the output and the input: $\Delta[\text{Output}] = \beta^T \cdot \Delta[\text{Input}]$. The amplifiers have been extensively used and are essential to modulate the signal carriers in the form of voltage or current in electrical and electronic systems. However, there are no such high-order devices in our current toolbox for the design of new biological systems which can predictably modulate the signal carriers in the form of messenger RNA and protein concentrations in cascaded gene networks.

To address such bottleneck in gene circuit engineering, we present the construction of modular genetic devices that function as *transcriptional amplifiers* in *Escherichia coli* bacteria, i.e. circuits that are able to scale up transcriptional signals within gene regulatory networks (10–12). The gain of the bio-amplifiers is rendered continuously tunable through the use of an external control signal (Figure 1A), thus allowing for dynamic tuning of cellular transcriptional processes (13). Being able to predictably scale a transcriptional signal affords a new level of control and flexibility over the outputs of genetic circuits where saturated or low threshold level transcription signals need to be scaled up for increased sensitivity or matching. Like their electronic counterparts, the engineered amplifiers are of critical value to customize signal processing in cells for various repurposed, beneficial applications.

We designed the genetic amplifier using orthogonal genetic components (*hrpRS*, *hrpV* and P_{hrpL}) from the *hrp* (hypersensitive response and pathogenicity) gene regulatory network for Type III secretion in *Pseudomonas syringae* (14–16). Strikingly, the natural gene regulatory architecture in the *hrp* control network contains the ingredients of a tunable transcriptional device (Figure 1B): the activator proteins HrpR and HrpS form a ultrasensitive high-order co-complex, which bind the upstream activator sequence of the σ^{54}-dependent *hrpL* promoter to re-

*To whom correspondence should be addressed. Tel: +0044-131-650-5527; Fax: +0044-131-650-8650; Email: Baojun.Wang@ed.ac.uk

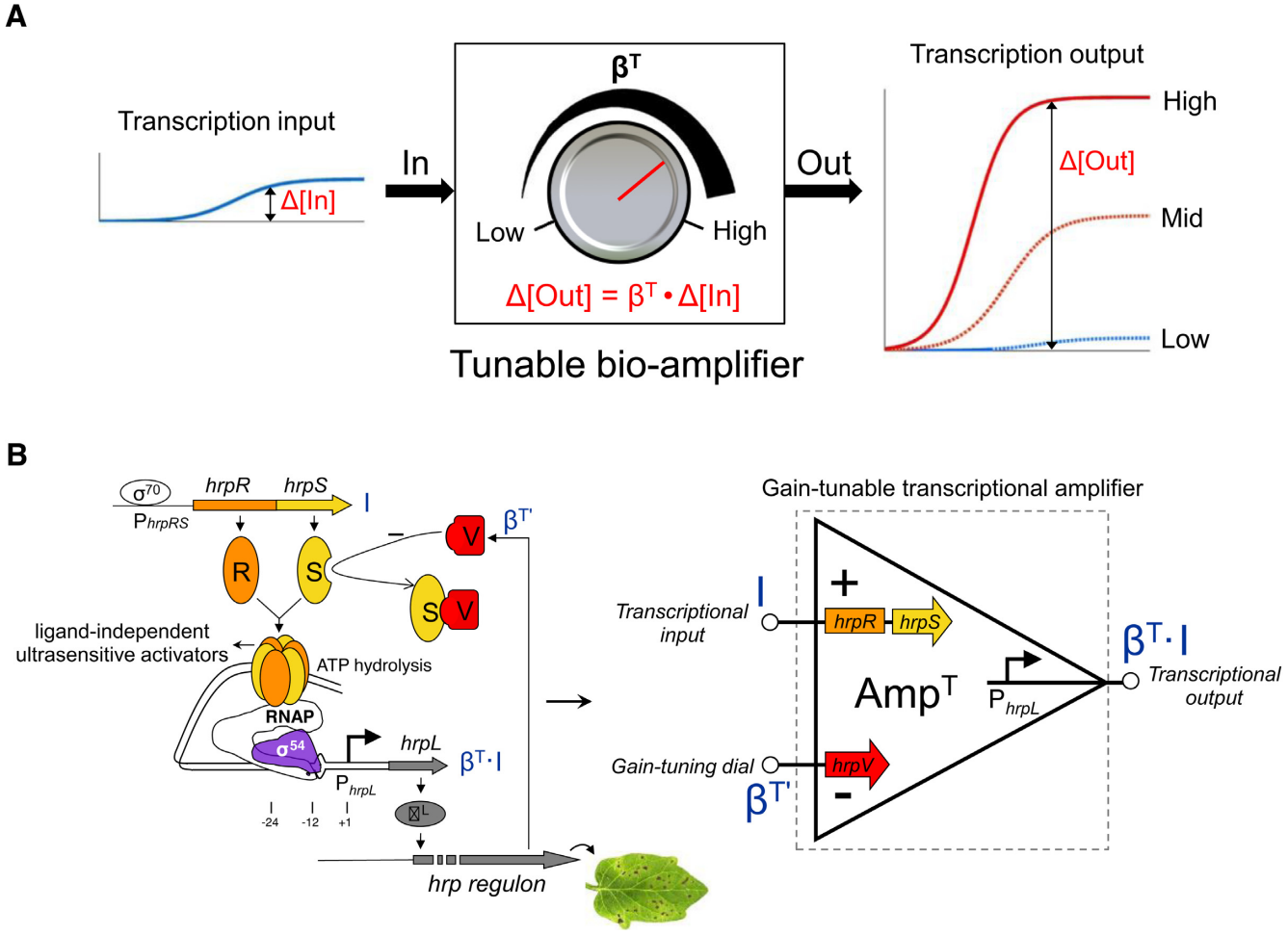

Figure 1. A modular and gain-tunable genetic amplifier design for the modulation of transcriptional signals in cascaded gene networks. (**A**) The tunable biological amplifier comprises three modular terminals—the input, the output and a gain-tuning input. The device can continuously process the input transcriptional signal in a defined analog mode with an externally tunable gain (the amplification ratio of the changes in output to input) control. (**B**) The architecture of the genetic amplifier. A tunable-gain transcriptional amplifier is designed on the basis of the transcriptional regulators HrpR (R), HrpS (S) and HrpV (V) in the *hrp* (hypersensitive response and pathogenicity) gene regulatory module from plant pathogen *P. syringae*.

model the closed σ^{54}-RNAP-*hrpL* transcription complex to an open one through ATP hydrolysis, while negative regulation by the inhibitor HrpV occurs through its interaction with HrpS (17). Using these regulatory components, we designed a three-terminal continuously tunable amplifier (Figure 1B) as well as the two-terminal fixed-gain amplifier (Figure 2A), which is a simplified case of the former. In contrast to other work based on the variation of regulatory sequences or extra-cellular ligand concentrations (18–20), our design controls the amounts of *in trans* acting protein components to achieve tunable transcriptional devices. To drive circuit outputs, we used transcription factors that function independently of any ligand binding, so as to avoid ligand saturation typical of simple transcriptional repressor and activator proteins. In particular, our set of genetic amplifiers achieves different gains and input dynamic ranges by varying the expression levels of the underlying ligand-free activator proteins in the device. Due to their modularity and orthogonality, these engineered devices can be readily introduced in various genetic networks to precisely tune transcriptional signal flow to implement advanced intra- and extra-cellular control functions.

MATERIALS AND METHODS

Plasmid circuit construction

Plasmid construction and deoxyribonucleic acid (DNA) manipulations were performed following standard molecular biology techniques. The *hrpR*, *hrpS*, *hrpV* genes, *hrpL* promoter and arsenic responsive sensor construct *arsR*-P_{arsR} were synthesized by GENEART following the BioBrick standard (http://biobricks.org) by eliminating the four restriction sites (EcoRI, XbaI, SpeI and PstI) for the BioBrick standard via synonymous codon exchange and flanking with prefix and suffix sequences containing the appropriate restriction sites and ribosome binding site (RBS) sequences. The double terminator BBa_B0015 (http://partsregistry.org) was used to terminate gene transcription in all cases. The arabinose inducible *araC*-P_{BAD} promoter was amplified from plasmid pBAD18-Cm (pBR322 ori, Cm^r). pSB3K3 (21) (p15A ori, Kan^r) was used to clone

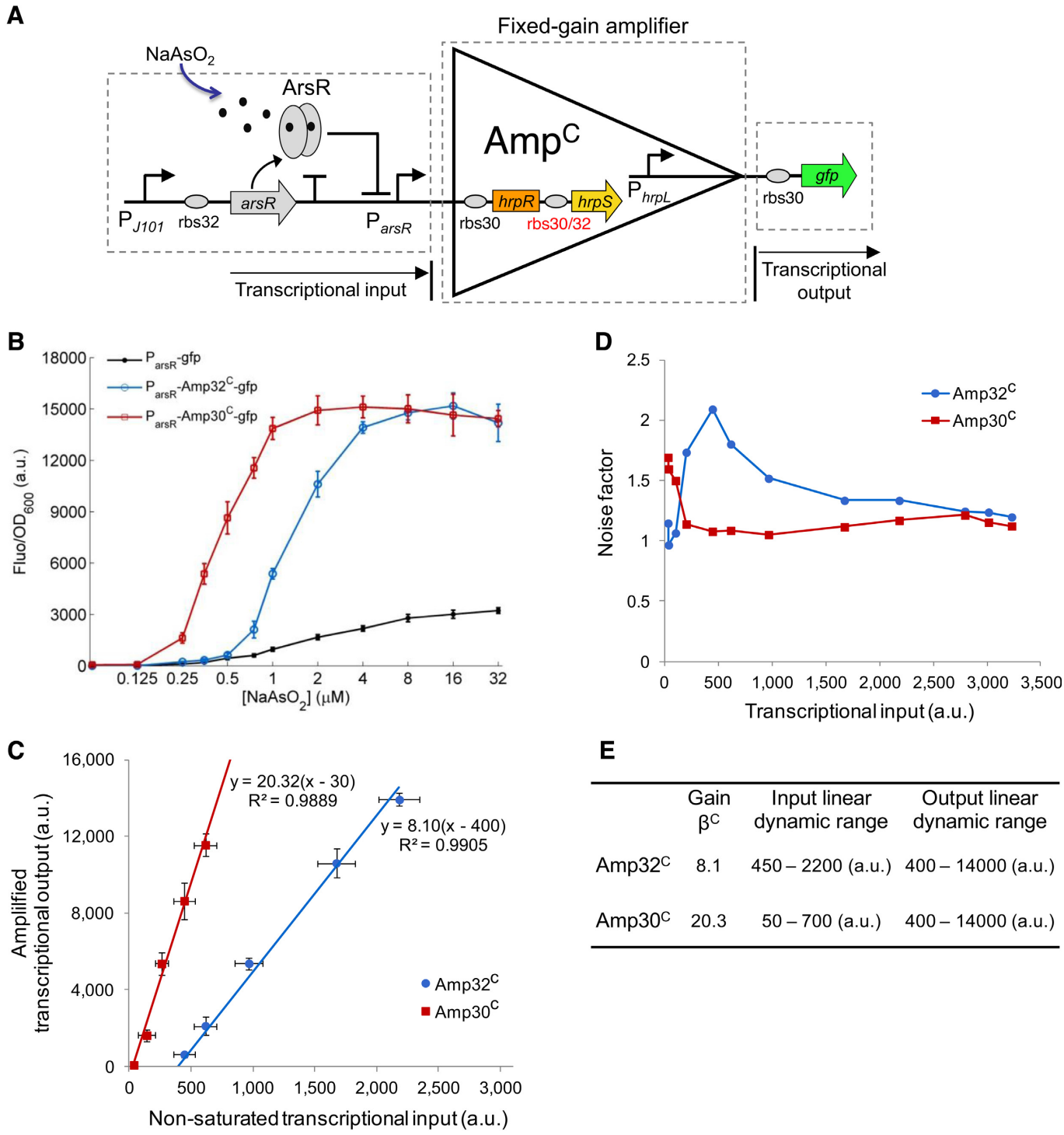

E

	Gain β^C	Input linear dynamic range	Output linear dynamic range
$Amp32^C$	8.1	450 – 2200 (a.u.)	400 – 14000 (a.u.)
$Amp30^C$	20.3	50 – 700 (a.u.)	400 – 14000 (a.u.)

Figure 2. Engineering and characterization of the fixed-gain amplifiers $Amp32^C$ and $Amp30^C$. (**A**) The fixed-gain transcriptional amplifier comprises two terminals corresponding to the signal input and signal output. Here two amplifiers with different gains, $Amp32^C$ and $Amp30^C$, are designed by using two different RBS sequences ahead of the *hrpS* gene. An arsenic responsive sensor is the input signal and *gfp* the output. (**B**) Steady state responses of the arsenic sensor without amplification and with amplification by $Amp32^C$ and $Amp30^C$. The cells are induced by 12 varying concentrations of arsenite (0, 0.125, 0.25, 0.35, 0.5, 0.75, 1.0, 2.0, 4.0, 8.0, 16, 32 μM $NaAsO_2$). (**C**) The scatter plot shows the linear relationships between the non-saturated transcriptional inputs (the signal inputs that do not lead to maximum output level of the device) and the amplified outputs of $Amp32^C$ and $Amp30^C$ by fitting to a linear function. (**D**) Device noise characteristics of $Amp32^C$ and $Amp30^C$. (**E**) Performance characteristics summary of the two amplifiers. Data shown in these figures are means and s.d. for three replicates performed on different days.

and characterize all the genetic constructs in this study. The GFP (Green Fluorescent Protein, *gfpmut3b*, BBa_E0840) reporter was from the Registry of Standard Biological Parts (http://partsregistry.org). The various RBS sequences (Supplementary Table S7) for each gene construct were introduced by polymerase chain reaction amplification (using PfuTurbo DNA polymerase from Stratagene and an Eppendorf Mastercycler gradient thermal cycler) with primers containing the corresponding RBS sequences and appropriate restriction sites. The constitutive promoters were assembled from two annealed single stranded primers flanked with appropriate restriction sites. All circuit constructs (Supplementary Table S8) were assembled following the BioBrick DNA assembly method and verified by DNA sequencing (Beckman Coulter Genomics) prior to their use. Primers were synthesized by Sigma Aldrich. Further information can be found in Supplementary Figures S16 and S17 (showing selected plasmid maps) and Supplementary Table S7 (part genetic sequences) describing the circuit constructs used. All plasmids used are available upon request and selected plasmids may be obtained from the the Registry of Standard Biological Parts (http://partsregistry.org).

Strains, media and growth conditions

Plasmid cloning work and circuit construct characterization were all performed in *E. coli* TOP10 strain. Cells were cultured in LB (Luria-Bertani broth) media (10 g/l peptone, 5 g/l NaCl, 5 g/l yeast extract). The kanamycin used was 50 μg/ml. Cells inoculated from single colonies on freshly streaked plates were grown overnight in 5 ml LB in sterile 20 ml universal tubes at 37°C with shaking (200 rpm). Overnight cultures were diluted into pre-warmed LB media at $OD_{600} = 0.025$ for the day cultures, which were induced (see below) and grown for 5 h at 37°C prior to analysis. For fluorescence assay by fluorometry, diluted cultures were loaded into a 96-well microplate (Bio-Greiner, chimney black, flat clear bottom) and induced with 5 μl (for single input induction) or 10 μl (for double input induction) inducers of varying concentrations to a final volume of 200 μl per well by a multichannel pipette. The microplate was covered by a UV transparent lid to counteract evaporation and incubated in the fluorometer (BMG FLUOstar) with continuous shaking (200 rpm, linear mode, 37°C) between each cycle of repetitive measurements. The growth curves of the cells containing various genetic constructs (Supplementary Figure S15) show that the devices engineered in this study did not impose any observable growth burden on the *E. coli* host. Chemical reagents and inducers (arabinose and sodium arsenite) used were of analytical grade from Sigma Aldrich.

Assay of gene expression

Fluorescence levels of gene expression were assayed by fluorometry at the cell population level and by flow cytometry at the single cell level. Cells grown in 96-well plates were monitored and assayed using a BMG FLUOstar fluorometer for repeated absorbance (OD_{600}) and fluorescence (485 nm for excitation, 520 ± 10 nm for emission, Gain = 1000, bottom reading) readings (20 min/cycle). Fluorescence-activated cell sorting (FACS) assay were performed using a Becton-Dickinson FACSCalibur flow cytometer with a 488-nm argon excitation laser and a 530-nm emission filter with 30-nm bandpass. After 5 h growth post the day culture dilution, cells were transferred from their 96-well plate and resuspended in 0.22 μm filtered phosphate buffered saline for FACS assay. The flow cytometer was tuned with the negative control (GFP-free) to obtain a fluorescence level centred within the first decade under log mode and the cells scatter at correct position on the scatter graph. Cells were assayed at low flow rate until 20,000 total events were collected using the BD CellQuest Pro software on a MAC workstation.

Modelling and data analysis

A deterministic approach was used with ODE (Ordinary Differential Equation)-based rate equations to model the gene regulation. The transfer functions for the biological modules were derived following a steady state assumption (Supplementary Methods). The non-linear least square fitting function (cftool or sftool) in Matlab (MathWorks R2010a) was applied to fit the experimental data to parameterize the transfer function models. In addition, an empirical mathematical model ($y = k \cdot (x - b)$) was used to fit selected data in the linear amplification range of the device. The fluorometry data of gene expression were first processed in BMG Omega Data Analysis Software (v1.10) and were analysed in Microsoft Excel 2007 and Matlab after being exported. The medium backgrounds of absorbance and fluorescence were determined from blank wells loaded with LB media and were subtracted from the readings of other wells. The fluorescence/OD_{600} (Fluo/OD_{600}) at a specific time for a sample culture was determined after subtracting its triplicate-averaged counterpart of the negative control cultures (GFP-free) at the same time. For population-averaged assay by fluorometry, the fluorescence/OD_{600} after 5 h growth post initial day dilution and induction was used as the output response of the cells in the steady state when cells were in exponential growth and the steady state assumption for protein expression is applied. For the constitutive promoter assay by fluorometry, the fluorescence values immediately after dilution were used as the baseline for the correction of subsequent fluorescence readings. The flow cytometry data were analysed using FlowJo software (v7.6) with an appropriate gate of forward-scattering and side-scattering for all cultures.

RESULTS

Engineering and characterization of the fixed-gain transcriptional amplifiers

The fixed-gain amplifier was built by expressing in an operon the cooperative activator proteins, HrpR and HrpS (17), whose high-order functional forms synergistically activate the downstream tightly controlled σ^{54}-dependent (22) *hrpL* promoter, thus assisting amplification (23) of the transcriptional input signal (Figure 2A). To obtain different amplification gains, two configurations of the amplifier ($Amp32^C$ and $Amp30^C$) were designed using two RBS sequences of distinct translational strengths (24) in front

of the *hrpS* gene. Amp30^{C}, with a strong RBS sequence (rbs30), should produce a higher signal gain than Amp32^{C} with a weaker RBS sequence (rbs32).

To verify their amplification capability, we connected an arsenic responsive transcriptional sensor (25) to the input of the fixed-gain amplifier with *gfp* as the output. By itself, the arsenic sensor generated a transcriptional output with limited dynamic range and sensitivity in response to varying levels of arsenite (Figure 2B and Supplementary Figure S1). When the transduced transcriptional input from the arsenic sensor was connected to our amplifier, the resulting output signal amplitude and dynamic range increased significantly as well as the response sensitivity to the inducer (Figure 2B) for both devices (Amp32^{C} and Amp30^{C}).

A Hill function-based biochemical model was derived to describe the amplifier transfer function (i.e. the transcriptional input–transcriptional output relationship) across the full operating range (Supplementary Methods, Figures S1–S3 and Tables S1 and S2). This transfer function displays a linear amplification operating range (Supplementary Figures S2B and S3B) that yielded an amplification gain of 8.1 for Amp32^{C} and a higher gain of 20.3 for Amp30^{C} (Figure 2C), as expected. Note that the two amplifiers have different but complementary linear input dynamic ranges and similar linear output dynamic range (Figure 2E). Hence the higher gain Amp30^{C} is more appropriate to amplify weak transcriptional signals (50–700 a.u.), while the lower gain Amp32^{C} is more suited to amplify middle range transcriptional signals (450–2200 a.u.) while preventing output saturation.

Signal amplification dynamics and modularity of the fixed-gain amplifiers

To analyse the signal fidelity of the two fixed-gain amplifiers, we calculated their noise factors (26) (NF) against varying transcriptional signal inputs. The NF is the ratio between the input to output signal-to-noise ratios: $NF = SNR_{IN}/SNR_{OUT}$ (Supplementary Figure S4). The signal-to-noise ratio (SNR) is calculated from the single cell flow cytometry assays (Supplementary Figures S1C–S3C) as the ratio of the sample fluorescent mean to the standard deviation of the cell population: $SNR = \mu/\sigma$. SNR_{IN} is the SNR at the device input (arsenic sensor output without amplification) while SNR_{OUT} is the SNR at the device output (arsenic sensor output with amplification by Amp32^{C} and Amp30^{C}). Our results (Figure 2D) show that the SNR degraded mainly within the lower amplification range of the two amplifiers, corresponding to the slow (and noisier) transcriptional rate stage of the input promoter. However, the two fixed-gain amplifiers did not introduce significant sources of noise, with mild degradation of the SNR ($NF < 2$) across their full input operating ranges (27).

To determine if the amplifiers introduce a significant time delay in the generation of the output response, we tested the dynamic response of the two amplifiers by measuring their output fluorescence continuously over a 20-min interval. Comparison of the output fluorescence production rate of the arsenic sensor without amplification (Figure 3A) and those amplified by Amp32^{C} (Figure 3B) and Amp30^{C} (Figure 3C) suggested no significant time delay introduced by the two amplifiers, although clear differences are evident in their output production rates and response thresholds. Hence the potential delay introduced by the extra layer of signal amplification may be too short ($\sim$ a few minutes) to be detectable using GFP as the reporter.

To test the modularity of the amplifier, as well as the validity of its transfer function, we linked the amplifier downstream to a set of constitutive promoter inputs. Six constitutive promoters of varying transcriptional strengths were used to drive Amp32^{C} (Supplementary Figure S5). All six transcriptional inputs were amplified significantly (Figure 3D), and the signal gain for these promoter inputs within the linear amplification range was 6.47 (Figure 3E). This gain is broadly consistent with that measured under the arsenic sensor input (Figure 2E), thus confirming the modularity of the amplifier design.

Engineering and characterization of the tunable-gain transcriptional amplifiers

We next proceeded to construct a *tunable-gain amplifier* comprising three terminals: a signal input and a signal output as before, and a gain-tuning control input used to tune the amplification gain (Figure 4A). To achieve continuous amplification of the transcriptional input, we appended an extra modular terminal to control the expression of HrpV, an inhibitor of the *hrpL* output promoter directly interacting with HrpS to cause inhibition of HrpRS activity. Tuning the transcriptional input to this terminal thus controls the device output transcriptional production rate (28) to realize a tunable-gain function. As above, we designed two tunable amplifiers, Amp32^{T} and Amp30^{T}, using two RBS sequences of distinct translational strengths ahead of *hrpS* in order to achieve different signal gains. Again the design is kept modular: the two inputs and the output are a common transcriptional signal and can thus be coupled to various input and output genetic modules.

To characterize the two tunable amplifiers, we connected the arsenic transcriptional sensor to the input terminal and the arabinose inducible P_{BAD} promoter to the gain-tuning terminal, while *gfp* was linked to the output terminal (Figure 4 and Supplementary Figure S8). The devices were subsequently characterized using varying combinations of the two input inductions. The results show that both Amp32^{T} (Figure 4B) and Amp30^{T} (Supplementary Figure S8B) amplify the transcriptional input signal (indicated by arsenite induction) with their output amplitude continuously scaled down in proportion to the control input (indicated by arabinose induction). The single cell flow cytometry assay further illustrates that the cellular output responses were tuned across the whole cell population (Figure 4C and Supplementary Figure S8C).

A biochemical model was used to derive a transfer function of the tunable amplifier across the full operating range (Supplementary Methods and Table S2), with the resulting transfer functions of Amp32^{T} and Amp30^{T}, closely matching their experimentally determined behaviours (Supplementary Figures S10 and S11). The linear amplification of the two devices was then fitted to the input–output responses in the non-saturated operating range (Figure 4D, Supplementary Figure S8D and Tables S3–S5). Note that

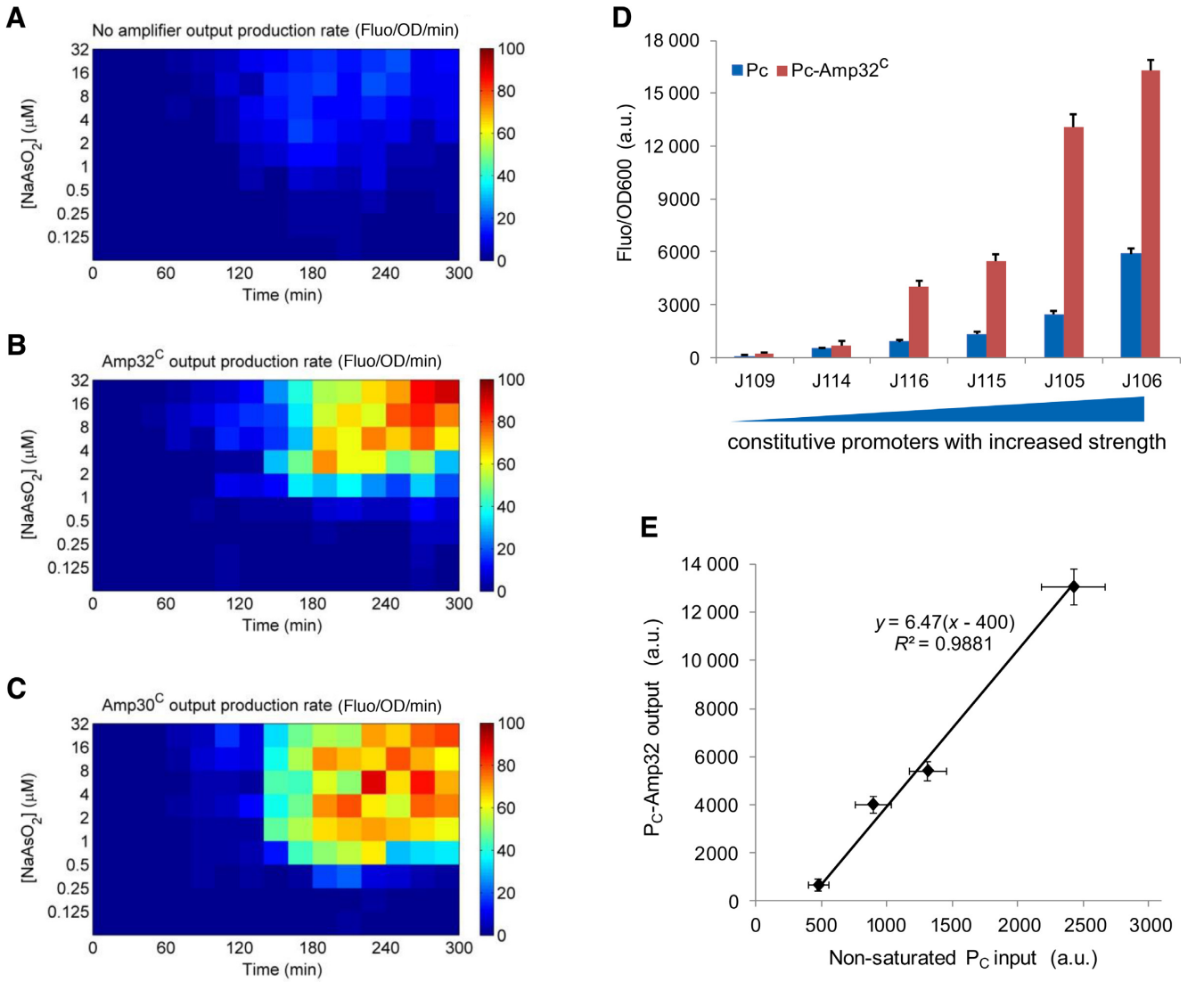

Figure 3. Signal amplification dynamics and modularity of the fixed-gain amplifier Amp32^{C}. Dynamic responses of the arsenic sensor without amplification (**A**), amplified by Amp32^{C} (**B**) and Amp30^{C} (**C**). (**D**) The performance of Amp32^{C} using a set of constitutive promoters as inputs and the *gfp* as output. Six constitutive promoters of varying transcriptional strengths are used—J109, J114, J116, J115, J105 and J106. The blue bars are the promoter output responses without the amplifier while the red bars are the ones amplified. (**E**) The scatter plot shows the linear relationship between the non-saturated transcriptional inputs (J114, J116, J115, J105) and the amplified outputs as in (D) by fitting to a linear model. Data are means and s.d. for three replicates.

the output responses under different gain-control levels are also highly correlated between themselves (Supplementary Figures S7 and S8E) confirming that the device operates as a three-terminal tunable-gain transcriptional amplifier whose amplification gain can be continuously tuned by the control input in a linear manner. The performance characteristics of Amp32^{T} and Amp30^{T}, summarized in Figure 4E, show that the two devices have different tunable-gain scopes and linear input dynamic ranges but display similar linear output dynamic ranges, and are thus complementary for the amplification of transcriptional signals of different amplitudes.

We next established that the tunable-gain amplifier is modular and so may be linked to any transcriptional input. Our experimental results using six constitutive promoters of different transcriptional strengths as the input for Amp32^{T} (Supplementary Figure S9) reveal that the characteristics and linear response regime remain consistent across different inputs (Supplementary Table S6), and that the obtained transfer function describes well the experimental data (Supplementary Figure S12).

DISCUSSION

Using orthogonal genetic components from *P. syringae*, we have designed and constructed modular and tunable biological amplifiers in *E. coli* that can scale transcriptional signals in a defined analog mode. To our knowledge, these are the first analog devices (29,30) capable of linearly amplifying *transcriptional signals* with a wide tunable-gain scope and a large output dynamic range. Moreover, the transcriptional amplifiers did not introduce obvious time delays (several minutes) and significant sources of noise during the signal amplification stage, which is important for modulating

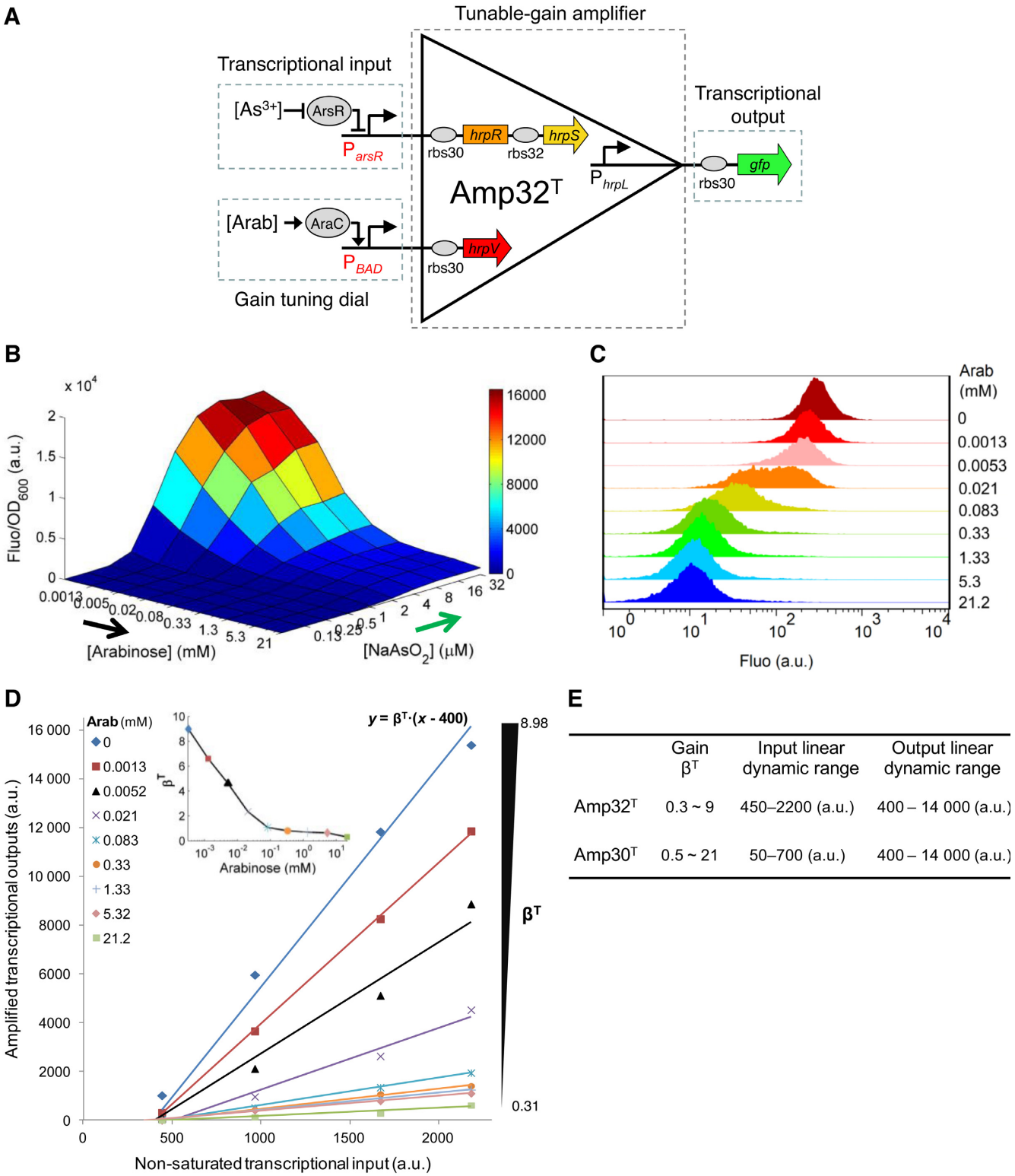

	Gain β^T	Input linear dynamic range	Output linear dynamic range
Amp32^T	0.3 ~ 9	450–2200 (a.u.)	400 – 14 000 (a.u.)
Amp30^T	0.5 ~ 21	50–700 (a.u.)	400 – 14 000 (a.u.)

Figure 4. Engineering and characterization of the tunable-gain amplifier Amp32^T. (**A**) The tunable amplifier Amp32^T comprises three modular terminals: transcriptional signal input, gain-tuning control input and transcriptional signal output. (**B**) The transfer function of Amp32^T under 90 combinations of two input inductions (0, 0.125, 0.25, 0.5, 1.0, 2.0, 4.0, 8.0, 16, 32 μM $NaAsO_2$ by 0, 1.3×10^{-3}, 5.2×10^{-3}, 2.1×10^{-2}, 8.3×10^{-2}, 0.33, 1.33, 5.32 and 21.2 mM arabinose). Data shown are means for three replicates on different days with variations less than 10% between repeats. (**C**) The single cell flow cytometry for cellular responses of the amplifier induced by 32 μM $NaAsO_2$ and different arabinose concentrations. (**D**) Scatter plot showing the linearity between the non-saturated transcriptional inputs and their amplified transcriptional outputs of Amp32^T under different gains as in (B) by fitting to a linear model. (**E**) Performance characteristics summary of Amp32^T and Amp30^T (Supplementary Figure S8).

biological signals because of their inherent slow dynamics and noisy characteristics (31). Due to the ligand independence of the main transcription factors used and to their modularity and orthogonality, these robust amplifiers can be introduced into a variety of gene regulatory networks to systematically amplify and modulate transcriptional signal flow for a broad range of biotechnological applications. For example, the devices can modulate the amplitude of an input signal to facilitate the coupling and matching of genetic modules with vastly different input–output strengths (32). The amplifiers can also be used to predictably increase the sensitivity and output dynamic range of transcription-based biosensors for enhanced environmental risk detection such as the weak arsenic sensor described in this study (Figure 2). Furthermore, the tunable-gain amplifiers could be readily placed within synthetic cellular metabolic pathways to precisely regulate pathway gene expression flow in response to either external (33) or endogenous metabolite signals (8,34) by coupling a relevant genetic sensor to the gain-tuning input.

The tunable genetic amplifier can also be thought of as a differential amplifier (9) whose output transcriptional signal is proportional to the *difference* between the input and the gain-tuning control input (Supplementary Figure S13A). By wiring the output to the gain-tuning input to form a negative feedback (Supplementary Figure S13B), the amplifier may thus be applied to realize robust adaptive sensing and gene expression control by autonomously tuning the output to stay at a constant level, independent of environmental or cellular context variations (35).

SUPPLEMENTARY DATA

Supplementary Data are available at NAR Online, including Supplementary Tables S1-S8, Supplementary Figures S1-S17, Supplementary Methods and References.

ACKNOWLEDGEMENT

We thank C. Simpson for the assistance on the flow cytometry experiment and T. Ellis for critical reading of the manuscript and valuable suggestions.

FUNDING

BBSRC project grants [BB/K016288/1] and [BB/G020434/1]; Royal Society grant award [RG120527] to B.W. Funding for open access charge: Research Councils UK (RCUK) for grant [BB/K016288/1].
Conflict of interest statement. None declared.

REFERENCES

1. Kiel,C., Yus,E. and Serrano,L. (2010) Engineering signal transduction pathways. *Cell*, **140**, 33–47.
2. Wang,B. and Buck,M. (2012) Customizing cell signaling using engineered genetic logic circuits. *Trends Microbiol.*, **20**, 376–384.
3. Moon,T.S., Lou,C., Tamsir,A., Stanton,B.C. and Voigt,C.A. (2012) Genetic programs constructed from layered logic gates in single cells. *Nature*, **491**, 249–253.
4. Callura,J.M., Cantor,C.R. and Collins,J.J. (2012) Genetic switchboard for synthetic biology applications. *Proc. Natl. Acad. Sci. U.S.A.*, **109**, 5850–5855.
5. Kemmer,C., Gitzinger,M., Daoud-El Baba,M., Djonov,V., Stelling,J. and Fussenegger,M. (2010) Self-sufficient control of urate homeostasis in mice by a synthetic circuit. *Nat. Biotechnol.*, **28**, 355–360.
6. Weber,W. and Fussenegger,M. (2012) Emerging biomedical applications of synthetic biology. *Nat. Rev. Genet.*, **13**, 21–35.
7. Topp,S. and Gallivan,J.P. (2007) Guiding bacteria with small molecules and RNA. *J. Am. Chem. Soc.*, **129**, 6807–6811.
8. Zhang,F., Carothers,J.M. and Keasling,J.D. (2012) Design of a dynamic sensor-regulator system for production of chemicals and fuels derived from fatty acids. *Nat. Biotechnol.*, **30**, 354–359.
9. Coughlin,R.F. and Driscoll,F.F. (2000) *Operational Amplifiers and Linear Integrated Circuits*. 6th ed. Prentice-Hall, New Jersey.
10. Gianna De,R. and Davies,S.W. (2003) A genetic circuit amplifier: design and simulation. *IEEE Trans. Nanobioscience*, **2**, 239–246.
11. Varadarajan,P.A. and Del Vecchio,D. (2009) Design and characterization of a three-terminal transcriptional device through polymerase per second. *IEEE Trans. Nanobioscience*, **8**, 281–289.
12. Nistala,G., Wu,K., Rao,C. and Bhalerao,K. (2010) A modular positive feedback-based gene amplifier. *J. Biol. Eng.*, **4**, 4.
13. Levskaya,A., Weiner,O.D., Lim,W.A. and Voigt,C.A. (2009) Spatiotemporal control of cell signalling using a light-switchable protein interaction. *Nature*, **461**, 997–1001.
14. Jin,Q., Thilmony,R., Zwiesler-Vollick,J. and He,S.-Y. (2003) Type III protein secretion in *Pseudomonas syringae*. *Microbes Infect.*, **5**, 301–310.
15. Hutcheson,S.W., Bretz,J., Sussan,T., Jin,S. and Pak,K. (2001) Enhancer-binding proteins HrpR and HrpS interact to regulate *hrp*-encoded type III protein secretion in *Pseudomonas syringae* strains. *J. Bacteriol.*, **183**, 5589–5598.
16. Buttner,D. and Bonas,U. (2006) Who comes first? How plant pathogenic bacteria orchestrate type III secretion. *Curr. Opin. Microbiol.*, **9**, 193–200.
17. Jovanovic,M., James,E.H., Burrows,P.C., Rego,F.G.M., Buck,M. and Schumacher,J. (2011) Regulation of the co-evolved HrpR and HrpS AAA+ proteins required for *Pseudomonas syringae* pathogenicity. *Nat. Commun.*, **2**:177.
18. Alper,H., Fischer,C., Nevoigt,E. and Stephanopoulos,G. (2005) Tuning genetic control through promoter engineering. *Proc. Natl. Acad. Sci. U.S.A.*, **102**, 12678–12683.
19. Egbert,R.G. and Klavins,E. (2012) Fine-tuning gene networks using simple sequence repeats. *Proc. Natl. Acad. Sci. U.S.A.*, **109**, 16817–16822.
20. Stricker,J., Cookson,S., Bennett,M.R., Mather,W.H., Tsimring,L.S. and Hasty,J. (2008) A fast, robust and tunable synthetic gene oscillator. *Nature*, **456**, 516–519.
21. Shetty,R., Endy,D. and Knight,T. (2008) Engineering BioBrick vectors from BioBrick parts. *J. Biol. Eng.*, **2**, 5.
22. Buck,M., Bose,D., Burrows,P., Cannon,W., Joly,N., Pape,T., Rappas,M., Schumacher,J., Wigneshweraraj,S. and Zhang,X. (2006) A second paradigm for gene activation in bacteria. *Biochem. Soc. Trans.*, **34**, 1067–1071.
23. Zhang,Q., Bhattacharya,S. and Andersen,M.E. (2013) Ultrasensitive response motifs: basic amplifiers in molecular signalling networks. *Open Biol.*, **3**, 130031.
24. Wang,B., Kitney,R.I., Joly,N. and Buck,M. (2011) Engineering modular and orthogonal genetic logic gates for robust digital-like synthetic biology. *Nat. Commun.*, **2**, 508.
25. Wang,B., Barahona,M. and Buck,M. (2013) A modular cell-based biosensor using engineered genetic logic circuits to detect and integrate multiple environmental signals. *Biosens. Bioelectron.*, **40**, 368–376.
26. Friis,H.T. (1944) Noise figures of radio receivers. *Proc. IRE*, **32**, 419–422.
27. Karki,J. (2003) Calculating noise figure in op amps. *Analog Applic. J.*, **4Q**, 31–37.
28. Bonnet,J., Yin,P., Ortiz,M.E., Subsoontorn,P. and Endy,D. (2013) Amplifying genetic logic gates. *Science*, **340**, 599–603.
29. Sohka,T., Heins,R.A., Phelan,R.M., Greisler,J.M., Townsend,C.A. and Ostermeier,M. (2009) An externally tunable bacterial band-pass filter. *Proc. Natl. Acad. Sci. U.S.A.*, **106**, 10135–10140.
30. Daniel,R., Rubens,J.R., Sarpeshkar,R. and Lu,T.K. (2013) Synthetic analog computation in living cells. *Nature*, **497**, 619–623.

31. Hooshangi,S., Thiberge,S. and Weiss,R. (2005) Ultrasensitivity and noise propagation in a synthetic transcriptional cascade. *Proc. Natl. Acad. Sci. U.S.A.*, **102**, 3581–3586.
32. Del Vecchio,D., Ninfa,A.J. and Sontag,E.D. (2008) Modular cell biology: retroactivity and insulation. *Mol. Syst. Biol.*, **4**, 161.
33. Milias-Argeitis,A., Summers,S., Stewart-Ornstein,J., Zuleta,I., Pincus,D., El-Samad,H., Khammash,M. and Lygeros,J. (2011) In silico feedback for *in vivo* regulation of a gene expression circuit. *Nat. Biotechnol.*, **29**, 1114–1116.
34. Dahl,R.H., Zhang,F., Alonso-Gutierrez,J., Baidoo,E., Batth,T.S., Redding-Johanson,A.M., Petzold,C.J., Mukhopadhyay,A., Lee,T.S., Adams,P.D. *et al.* (2013) Engineering dynamic pathway regulation using stress-response promoters. *Nat. Biotechnol.*, **31**, 1039–1046.
35. Cardinale,S. and Arkin,A.P. (2012) Contextualizing context for synthetic biology—identifying causes of failure of synthetic biological systems. *Biotechnol. J.*, **7**, 856–866.